A PRIORI ESTIMATION OF VARIANCE FOR SURVEYING OBSERVABLES

B. G. NICKERSON

November 1978

TECHNICAL REPORT
NO. 57

PREFACE

In order to make our extensive series of technical reports more readily available, we have scanned the old master copies and produced electronic versions in Portable Document Format. The quality of the images varies depending on the quality of the originals. The images have not been converted to searchable text.

A PRIORI ESTIMATION OF VARIANCE FOR SURVEYING OBSERVABLES

B.G. Nickerson

Department of Geodesy and Geomatics Engineering
University of New Brunswick
P.O. Box 4400
Fredericton, N.B.
Canada
E3B 5A3

November 1978
Latest Reprinting January 1998

ACKNOWLEDGEMENTS

This work was partially funded by contract no. 132 730 from the Land Registration and Information Service to the University of New Brunswick. The help provided by Dr. D.B. Thomson during the writing of this report was particularly invaluable. The comments supplied by Dr. A. Chrzanowski are also appreciated. Ms. S. Biggar is acknowledged for her excellent typing.

TABLE OF CONTENTS

1. INTRODUCTION 1

2. ANGULAR MEASUREMENTS 3

2.1 Internal 3

2.1.1 Pointing Error 3
2.1.2 Reading Error 5
2.1.3 Leveling Error 6
2.1.4 Summary of Internal Accuracy 8

2.2 External 11

2.2.1 Zenith angles 11

2.2.1.1 Empirically Determined Refraction Angle .. 12
2.2.1.2 Simultaneous Reciprocal Zenith Angles. ... 14
2.2.1.3 Analytically Determined Refraction 15
2.2.1.4 Height of Target 16

2.2.2 Horizontal Angles 16

2.3 Other Error Sources Encountered for Azimuths 19

2.3.1 Gyro Azimuths 19
2.3.2 Azimuths Determined from Star Obersvations . . . 21

2.4 Summary 25

2.4.1 Directions 25
2.4.2 Horizontal Angles 26
2.4.3 Zenith Angles 28
2.4.4 Astronomic Azimuths 29
2.4.5 Geodetic Azimuths 29
2.4.6 "Grid" Azimuths 30

3. DISTANCE MEASUREMENTS 30

3.1 EDM 30

3.1.1 Internal 31
3.1.2 External 35
3.1.3 Summary of Variance for EDM 41

3.2 Mechanical Distance Measurement 42

3.3 Optical Distance Measurement 44

3.3.1 Stadia Tacheometry 44
3.3.2 Subtense Bar 46

3.4 Summary 48

LIST OF FIGURES

Figure 2.1 Zenith Angle Measurement 11

Figure 2.2 Reciprocal Zenith Angles 14

Figure 2.3 Effect of Lateral Refraction 17

Figure 2.4 Angles and Directions 27

Figure 3.1 Reduction of Distances 38

Figure 3.2 Tape in Catenary 43

Figure 3.3 Stadia Measurements 45

Figure 3.4 Bar at End 46

Figure 3.5 Bar in the Middle 47

Figure 3.6 Auxiliary Base at End 47

Figure 3.7 Auxiliary Base in the Middle of the Line 48

Figure 3.8 Expected Relative Precision of Subtense Bar Measurements . . 49

LIST OF TABLES

Table 2.1 Major Features of Some Modern Theodolites 4

Table 2.2 Internal Accuracy Default Values 9

Table 2.3 Expected Centering Error 18

Table 3.1 EDM Instruments 32

Table 3.2 Effect of Meteorological Errors on Measured Distances 37

1. INTRODUCTION

Observational accuracy in contemporary surveying practice is characterized by the standard derivation or variance of individual observations. In order that useful statistical propagation of this error can occur, these variances are assumed to have a normal distribution with zero mean. This implies that the variances must be composed of random errors, and that any error or inaccuracy which is systematic in nature has already been accounted for and removed, either by solving for the systematic component through an adjustment process, eliminating it through appropriate observation procedures, or eliminating it by other empirical techniques.

This report is intended to provide an analysis of the random errors inherent in observations encountered in surveying, which are used to estimate the variances of these observations. It must be made clear from the outset that the systematic errors encountered in surveying measurements are not considered directly. They are, however, given the attention necessary to evaluate the effect of errors made in eliminating or minimizing these systematic biases. This is necessary to compute realistic variances for the individual observations.

With this in mind, the errors are split into 2 distinct sections. The first covers random errors encountered when making angular measurements. The accuracy of directions, vertical and horizontal angles, and azimuths are all examined, although, as one would expect, they are very much interrelated. The second section deals with the random errors encountered when measuring distances. The accuracy of various electromagnetic distance measuring (EDM) equipment as well mechanical (e.g. chain) and optical methods are treated.

Only these basic surveying observables are analysed, and observations such as inertial, Doppler or hydrographic (e.g. range-range) measurements are not covered.

2. ANGULAR MEASUREMENTS

The term angular accuracy, in this report, refers to the accuracy of making measurements with a modern theodolite such as a Wild T2 or Kern DKM2. Various types of theodolites are available, and Table 2, [Cooper 1971] gives an excellent summary of the major features of some of the theodolites in use today.

This work does not intend to describe or assess the mechanical or optical components of theodolites. It is assumed that either the theodolite is in correct adjustment, or that any misalignment or other error can be eliminated by suitable observation procedures (e.g. mean of face left and face right readings corrects for line of collimation not being perpendicular to the axis of the theodolite). For those who are interested in theodolite construction, and its detailed analysis, an excellent reference is Cooper [1971]. Instead, the topics dealt with are concerned with random errors which are unavoidable in the everyday use of theodolites, and with obtaining reasonable estimates for them.

2.1 Internal

Internal errors are those which are caused by the actual equipment and/or observer using it. Errors considered under this heading include pointing, reading and levelling errors.

2.1.1 Pointing Error

The pointing error σ_p is directly related to the telescope magnification of the individual theodolite. Chrzanowski [1977] states that the maximum accuracy of pointing is 10"/M, where M is the telescope magnification. He

INSTRUMENT	MANUFACTURER	COUNTRY	Telescope					H. Circle		V. Circle		Reading		Spirit Levels Value of 2 mm			Weight (kg)
			Magnification	Objective diam(mm)	Length (mm)	Shortest Focus (m)	Field of View (°)	Diam. (mm)	Graduation	Diam. (mm)	Graduation	Direct to	System	Plate (")	Altitude (")	Spherical (')	
FT1A	Fennel	W. Germany	30	40	175	1.2	1.6	90	1°	70	1°	1'	Opt. Scale	40	auto.	8	4.0
DKM-1	Kern	Switzerland	20	30	120	0.9	1.7	50	20'	50	20'	10"	Opt. micro	30	30	-	1.8
K1-A	Kern	Switzerland	28	45	155	1.8	1.5	89	1°	70	1°	20"	Opt. micro	40	auto.	-	4.2
Te-E6	Mom	Hungary	20	28	123	1.3	2.0	80	20'	40	20'	10"	Opt. micro	50	auto.	6	2.6
Microptic 1	Rank	U.K.	25	38	146	1.6	1.5	89	20'	64	20'	20"	Opt. micro	40	30	-	4.5
4149-A	Salmoiraghi	Italy	30	36	172	2.0	1.4	90	30"	90	30"	30"	Direct	30	auto.	10	4.7
V22	Vickers	U.K.	25	38	137	1.8	2.0	78	1°	63	1°	20"	Opt. scale	45	90	17	5.2
T16	Wild	Switzerland	28	40	150	1.4	1.6	79	1°	79	1°	1'	Opt. scale	30	30	8	4.5
T1A	Wild	Switzerland	28	40	150	1.4	1.6	73	1°	65	1°	20"	Opt. micro	30	auto.	8	5.0
Theo 020	Zeiss(Jena)	E. Germany	25	35	195	2.1	1.6	96	1°	74	1°	1'	Opt. scale	30	auto.	8	4.3
Th 3	Zeiss(Ober.)	W. Germany	25	35	150	1.2	1.7	78	1°	70	1°	30"	Opt. micro	30	auto.	15	3.5
Th 4	Zeiss(Ober.)	W. Germany	25	35	150	1.2	1.7	98	1°	85	1°	1'	Opt. scale	30	auto.	10	4.5
Tu	Askania	W. Germany	30	45	165	1.5	1.6	90	20'	70	20'	1"	Coinc. micro	20	auto.	10	4.6
FT 2	Fennel	W. Germany	30	45	174	2.0	1.6	93	20'	60	20'	1"	Coinc. micro	20	20	6	5.5
DKM 2	Kern	Switzerland	30	45	170	1.7	1.3	75	10'	70	10'	1"	Coinc. micro	20	20	-	3.6
DKM 2-A	Kern	Switzerland	30	45	170	1.7	1.3	75	10'	70	10'	1"	Coinc. micro	20	auto.	-	6.8
TB-1	Mash-priboritorg	USSR	26	40	180	1.2	1.3	85	20'	75	20'	1"	Coinc. micro	20	25	12	5.1
Te-B3	Mom	Hungary	30	40	175	2.5	1.5	78	20'	66	20'	1"	Coinc. micro	20	auto.	6	5.5
Microptic 2	Rank	U.K.	28	41	165	1.8	1.5	98	10'	76	10'	1"	Coinc. micro	20	20	-	6.3
4200-A	Salmoiraghi	Italy	30	40	172	2.5	1.5	40	10'	90	10'	1"	Coinc. micro	20	auto.	10	6.1
Tavistock 2	Vickers	U.K.	25	38	159	1.8	2.0	85	20'	70	20'	1"	Coinc. micro	20	20	20	4.8
T2	Wild	Switzerland	28	40	150	1.5	1.6	90	20'	70	20'	1"	Coinc. micro	20	30	8	5.6
Theo 010	Zeiss(Jena)	E. Germany	31	53	135	2.0	1.2	84	20'	60	20'	1"	Coinc. micro	20	20	8	5.3
Th2	Zeiss (Ober.)	W. Germany	30	40	155	1.6	1.3	100	10'	85	10'	1"	Coinc. micro	20	auto.	10	5.2
DKM3	Kern	Switzerland	27,45	72	140	19	1.6	100	10'	100	10'	0".5	Coinc. micro	10	10	-	12.2
DT-02	Mash-priboritorg	USSR	24,30, 40	60	265	5.0	1.6	135	4'	90	8'	0".2	Coinc. micro	7	12	-	11.0
Microptic 3	Rank	U.K.	40	50	170	1.8	1.0	98	5'	76	5'	0".2	Coinc. micro	10	20	-	8.0
Geod. Tavi.	Vickers	U.K.	20,30	60	225	5.0	1.3	127	20'	70	20'	0".5&1"	Coinc. micro	20	10	-	9.8
T3	Wild	Switzerland	24,30 40	60	265	3.6	1.6	135	4'	90	8'	0".2	Coinc. micro	7	30	-	11.2
T4	Wild	Switzerland	70	60	-	100	-	240	2'	135	4'	0".1/0".2	Coinc. micro	1	2	8	60

Table 2.1 Major Features of Some Modern Theodolites

further states that this minimum error is increased by improper target design, imperfect atmospheric conditions and focussing error. In average visibility and thermal turbulance conditions with a well designed target, one can expect a pointing error of

$$\sigma_p = \frac{30"}{M} \quad \text{up to} \quad \sigma_p = \frac{60"}{M} \tag{2-1}$$

for a single pointing at distances larger than a few hundred meters. Roelofs [1950] is in substantial agreement as he concludes that the accuracy of pointing on a star is $\sigma_p = 70"/M$ for either the horizontal or vertical crosshair. This seems reasonable considering that pointing on a moving star is not as accurate as pointing on a stationary target.

One can expect, then, to obtain the above error due to pointing in average conditions. The pointing error is partially due to personal error, and procedures outlined in section 2.1.4 enable one to determine the pointing error as well as the other internal errors discussed here. One can expect the pointing error to be larger when poor visibility or large thermal turbulence (e.g. scintillation) occur.

2.1.2 Reading Error

Reading error σ_r is primarily a function of the least count or smallest angular division of the theodolite. Error is also introduced if there are graduation errors in either the horizontal circle or the micrometer scale (for those theodolites which have micrometers). These graduation errors are assumed to be negligible due to observation procedures designed to

minimize them (i.e. taking the mean of many evenly spaced "zeros" between 0° and 180° for the horizontal circle, and using the full range of the micrometer scale for measurement of an individual set of directions (for instance)). Chrzanowski [1977] gives the following breakdown of reading errors for various types of readout systems:

1) theodolites with optical micrometers and with smallest division d of 1" or 0.5" : $\sigma_r = 2.5d"$. (2-2)

2) theodolites with a microscope to estimate the fraction of the smallest division (typically d = 10" to 1') : $\sigma_r = 0.3d"$. (2-3)

3) vernier theodolites with 2 verniers: $\sigma_r = 0.3d"$, where d" is the angular value of the vernier division.

The reason for σ_r being 2.5d for the optical micrometer as compared to 0.3d for direct reading instruments is because of inherent inaccuracies in operation of the optical micrometer. Cooper [1971] quotes an investigation which showed reading differences up to 10" over the 10' range of the micrometer of a 1" theodolite. Robbins [1976] states the reading error of a WILD T4 as 0".3 (its least count is 0".1) and that of the T3 as being 0".6, so this is in essential agreement with the findings of Chrzanowski.

It should be realized that the above estimates are based on the average ability to read these various readout systems. Personal error may affect this error significantly, and should be determined individually as discussed in section 2.1.4.

2.1.3 Levelling Error

The principal source of inaccuracy in levelling the instrument stems from the insensitivity of the spirit levels. The sensitivity of

spirit levels is characterized by their bubble value, which is the angular value necessary to displace the bubble through 1 of the divisions marked on the top of the spirit level. These divisions are usually placed 2 mm apart [Cooper, 1971]. Both Chrzanowski [1977] and Cooper [1971] state that it is possible to center the bubble to an accuracy of about 1/5 of one division. Thus, for a bubble value v", the accuracy that can be expected for levelling the spirit level is

$$\sigma_v = 0.2\ v" \ . \qquad (2\text{-}4)$$

This value is, of course, only valid for good conditions (i.e. one side of the theodolite not heated more than the other side, stable tripod, spirit level correctly adjusted, etc.). The bubble values of various theodolites are listed in Table 2.1.

A spirit level which is centered by a coincidence reading system (i.e. split bubble) is, according to Cooper [1971], able to be centered ten times as accurately as by viewing the bubble directly. Thus, a split bubble centering system, which is used by many manufacturers on the vertical circle bubble, has a levelling accuracy of

$$\sigma_v = 0.02\ v". \qquad (2\text{-}5)$$

Many present day theodolites have automatic compensators for the vertical circle. Cooper [1971] states that most 20" instruments claim an accuracy $\sigma_v = 1".0$ and that the Kern DKM2-A has $\sigma_v = 0".3$. One method of determining the accuracy of compensation is to take various readings of the vertical angle on a fixed target, each time moving one of the footscrews in order to take the compensator through its full working range. After removing the effects of reading and pointing errors, the resulting spread of readings will be due to the automatic compensation.

The above discussion of the error in levelling has been concerned with the accuracy levelling the instrument itself. What is of real concern is how this inaccuracy affects the actual angular accuracy of one pointing of the theodolite. Cooper [1971] and Chrzanowski [1977] both concur that the levelling inaccuracy has an effect of

$$\sigma_L'' = \sigma_v'' \cot h \qquad (2\text{-}6)$$

on a measured direction, where

h = zenith angle to target.

Thus, for small vertical angles, σ_L is negligible, but for steep lines of sight, σ_L is an increasing source of error.

2.1.4 Summary of Internal Accuracy

In concluding this section, the internal accuracy is given as

$$\sigma_i^2 = \sigma_p^2 + \sigma_r^2 + \sigma_L^2 , \qquad (2\text{-}7)$$

for one pointing of the telescope, and this figure is dependent on the instrument being used as well as the personal biases of the individual user.

The method used in the North American Readjustment [Pfeifer, 1975] as well as in the Maritime Provinces Second Order Readjustment [Chamberlain, 1977] is to compute the internal error for each mean direction in the sets

of directions at each station by means of a station adjustment [Mepham, 1976]. This analytical method gives a good estimate of the internal accuracy achieved for each individual direction, but is still composed of the 3 elements discussed above. Some default values of internal accuracy for typical types of surveys are given by Pfeifer [1975], and are listed here in table 2.2.

Order of Survey	Class of Survey	Nominal Relative Accuracy	Internal Accuracy σ_i
1		1:100 000	0".33
2	1	1:50 000	0".33
2	2	1:20 000	0".47
3	1	1:10 000	0".69
3	2	1:5 000	1".39

Table 2.2 Internal Accuracy Default Values

The final part of this section will describe a method which enables one to compute the expected reading, pointing and levelling errors for a particular theodolite and observer. The procedure is essentially the same as that carried out in a lab for course SE 3022 taught by Dr. Chrzanowski at the University of New Brunswick. The initial steps are to set up the instrument and tripod in normal conditions (e.g. outside on a cool day on a grassy slope) and center it over some point. The following steps then enable one to determine the reading, pointing and levelling accuracy:

1) Take 20 different readings of the same pointing. All that this involves is the setting of the coincidence of the vernier or micrometer hairs, and reading the setting 20 separate times. By taking the mean of the 20 readings and computing the standard deviation, one arrives at the reading error σ_r.

2) Take 20 different pointings and readings combined. This involves pointing the cross hairs on a stationary target, making a reading, moving the cross hairs off the target, pointing and reading again, etc. The standard deviation of these will give the combined pointing and reading error $\sqrt{\sigma_r^2 + \sigma_p^2}$ and by the law of propagation of errors, the pointing error is computed as

$$\sigma_p^2 = (\sigma_r^2 + \sigma_p^2) - \sigma_r^2 . \qquad (2\text{-}8)$$

3) The same pointings and readings are made as in step 2, except that now the instrument is thrown off level between each pointing and reading, and relevelled before each one. As already mentioned, this error should be negligible for small vertical angles, and the instrument in correct adjustment, but it would serve to estimate the levelling error if one was expecting to measure steep lines of sight. This standard deviation of these readings will yield the combined reading, pointing and levelling error, and σ_L is computed as

$$\sigma_L^2 = (\sigma_r^2 + \sigma_p^2 + \sigma_L^2) - (\sigma_r^2 + \sigma_p^2) . \qquad (2\text{-}9)$$

4) The centering error, which is discussed in section 2.2, can also be determined in this procedure. The same steps as carried out in step 3) are performed for each reading, except that now, the instrument and

tribrach together are turned through 120° and recentered between each reading. This set of readings will yield the combined centering, reading, pointing and levelling error, and by subtracting the variance obtained from 3) from the variance of the readings of 4), the accuracy of centering can be determined.

2.2 External

External inaccuracies stem from uncertainties in the determination of environmental factors such as refraction. As well, inaccuracies which are proportional to the distance between stations, although not strictly environmentally dependent, are included here. As can be expected, zenith angles are affected differently by the environment than are horizontal angles; thus, this section is divided into these two categories.

2.2.1 Zenith Angles

The primary cause of random error in zenith angles is the inaccuracy in determination of the vertical refraction. As indicated in Figure 2.1, refraction causes the ray of light between two stations to be curved, thus causing the desired zenith angle z to be in error

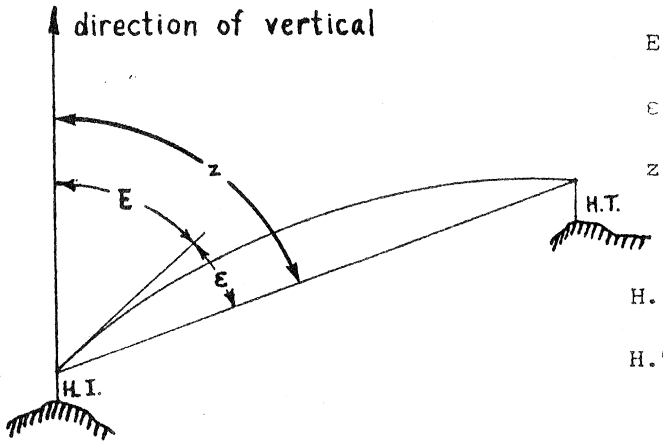

E = measured zenith angle

ε = refraction angle

z = required zenith angle

H.I. = height of instrument

H.T. = height of target

Figure 2.1 Zenith Angle Measurement

by ε. The random error in the zenith angle z is

$$\sigma_z^2 = \sigma_E^2 + \sigma_\varepsilon^2 \quad , \tag{2-10}$$

assuming no correlation between E and ε. The inaccuracies involved in determining E have already been discussed in the previous section, so the problem remains to determine σ_ε^2. This will depend on the method used to determine or eliminate the refraction angle ε. The 3 basic methods presently used to handle vertical refraction are

1) Add the empirically determined refraction angle to the observed zenith angle E.
2) Measure simultaneous reciprocal zenith angles to eliminate the effect of the refraction angle.
3) Model the vertical refraction into an adjustment including measured zenith angles to determine ε analytically.

2.2.1.1 Empirically Determined Refraction Angle

If the vertical or zenith angle is measured from only one end of the observing line, the refraction angle must be determined by empirical methods. This is usually accomplished by use of the coefficient of refraction k in the relationship [e.g. Faig, 1972]

$$\varepsilon = \frac{ks}{2R} \quad , \tag{2-11}$$

where k = coefficient of refraction,

s = distance between the 2 stations,

R = mean radius of curvature of the earth between the 2 stations.

The primary inaccuracy in (2-11) stems from inadequate knowledge of k, and thus

$$\sigma_\varepsilon^2 = \left(\frac{S}{2R}\right)^2 \sigma_k^2 . \qquad (2\text{-}12)$$

The coefficient of refraction can be computed as [Angus-Leppan, 1971]

$$k = 502 \frac{P}{T^2} \left(0.0341 + \frac{\partial T}{\partial h}\right) , \qquad (2\text{-}13)$$

where P = air pressure in millibars,

T = temperature in degrees Kelvin,

$\frac{\partial T}{\partial h}$ = temperature gradient in degrees Celcius per meter.

The temperature gradient in (2-13) is the most difficult item to ascertain. Angus-Leppan [1971] quotes values of -4°C/m for heights of 1 cm to 1 m above ground, -0.8° C/m from one metre to 2 metres above the surface, and -0.03° C/m from 2 to 100 m above ground for the temperature gradient on a clear summer day over grassland. The temperature gradient is a function of many things including density of the air, temperature, soil characteristics under the sight line, wind speed, etc. (see Angus-Leppan [1971]), but when observing lines are high above the ground at mid-day or afternoon, the values of $\partial T/\partial h$ approaches -0.0055, which corresponds to a value for k of 0.13. Investigations carried out by Angus-Leppan [1961] to determine an empirical formula for ε by measuring temperature gradients along lines of sight close to the ground (i.e. 5 feet to 30 feet) resulted in an accuracy of no better than σ_ε = 5" for a sight line 3600 feet long, which is an accuracy of about 4".5/km. It is apparent that the empirical method of determination of k is not accurate (using present instrumentation) even in the best of situations. Work is presently being carried out [Bomford, 1975] to determine the refraction directly by measuring the dispersion of two different coloured light beams, but it is still in the development stages.

2.2.1.2 Simultaneous Reciprocal Zenith Angles

This method of accounting for refraction is depicted in Figure 2.2.

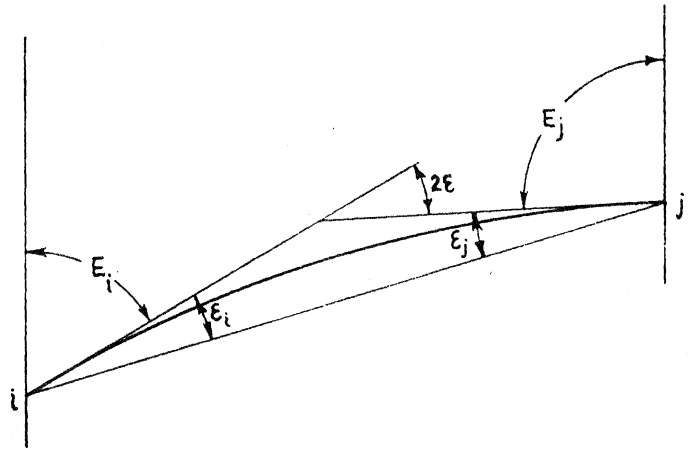

Figure 2.2 Reciprocal Zenith Angles

The basic assumption is that the refraction angle ε will be the same at both ends of the line ij, and thus

$$E_i + E_j + 2\varepsilon = 180^\circ \,, \tag{2-14a}$$

and

$$\varepsilon = \frac{180^\circ - (E_i + E_j)}{2} \,. \tag{2-14b}$$

The accuracy here depends on the validity of the assumption that the directions of the verticals at i and j are parallel in the plane of the line of observation between i and j. This assumption is valid for lines which are not too long (e.g. < 10 km) and which are not in a gravity disturbed area. Ramsayer [1978] reports an accuracy of 0.9" when measuring reciprocal zenith angles in 6 sets and accounting for the deflection of the vertical at each station. Thus, for 3 sets of zenith angles as each end, and assuming deflections of the vertical differences insignificant,

one would expect $\sigma_\varepsilon \approx 2''$.

Another slightly different approach to simultaneous reciprocal zenith angles is using only one theodolite, measure the zenith angle at one end, move the instrument to the other end of the line and observe the zenith angle at that end. This results in a time lag of about 10 min (depending on the distance between stations) between zenith angle measurements. A study done by Mepham [1977] of 278 lines of average length 250 m gives a standard deviation for the coefficient of refraction k of $\sigma_k = 1.86$, which results in $\sigma_\varepsilon = 7''.5$.

2.2.1.3 Analytically Determined Refraction

This method involves solving directly for the coefficient of refraction in an adjustment. Zenith angle observations are usually only considered directly in a three dimensional adjustment, and thus this procedure is usually only employed there. Vincenty [1973] introduces the term

$$\frac{-s}{10^3}\varepsilon \quad , \tag{2-15}$$

where s = distance from i to j,

and ε = refraction angle in arcsecs per kilometer,

into the observation equation for vertical angles in order to account for vertical refraction. Assuming an accuracy of 2" for zenith angle measurement and 0".7 for astronomic latitude and longitude in a ficticious network he arrives at an accuracy of 0".06 per km for ε. As already mentioned in 2.2.1.2, Ramsayer [1978] calculates an accuracy σ_ε of 0".9 independent of the length of the line in an actually measured network of 5 stations. This implies that the accuracy of the coefficient of

refraction is increasing with the length of the line, and Ramsayer [1978] gives the accuracy as $\sigma_k = 0.055 /s$ (km).

It seems that this method gives the best estimate for the refraction angle as it is determined by the least squares adjustment process itself.

2.2.1.4 Height of Target

The uncertainty in the height of target σ_{HT} affects the variance of a zenith angle observation, depending on the distance between stations. It is analagous to the centering error discussed in the next section. The angle δ contributed by the height of target to the zenith angle is

$$\delta = \frac{HT \sin E}{s}, \qquad (2\text{-}16)$$

where HT = height of target,

E = measured zenith angle,

and s = spatial distance between the 2 stations.

Thus, an error σ_{HT} in the height of target produces an error in δ of $\sigma_\delta = \frac{\sin E}{s} \sigma_{HT}$. For σ_{HT} of 1 cm, a zenith angle of 90° and a distance s of 1 km, $\sigma_\delta = 2''.06$.

2.2.2. Horizontal Angles

External effects considered for horizontal angles include lateral refraction, centering error and tripod twist. Of these, the only one which can be accounted for with any degree of accuracy is the centering error.

Lateral or horizontal refraction affects horizontal angles when the lines of sight pass close to objects which are significantly different in temperature than the surrounding air. Figure 2.3 [Kukkamaki, 1949] shows

the deflection of a 5.2 km line of sight which passed at 20 m height along a sideward slope. The line of sight passes about 3" closer to the ground

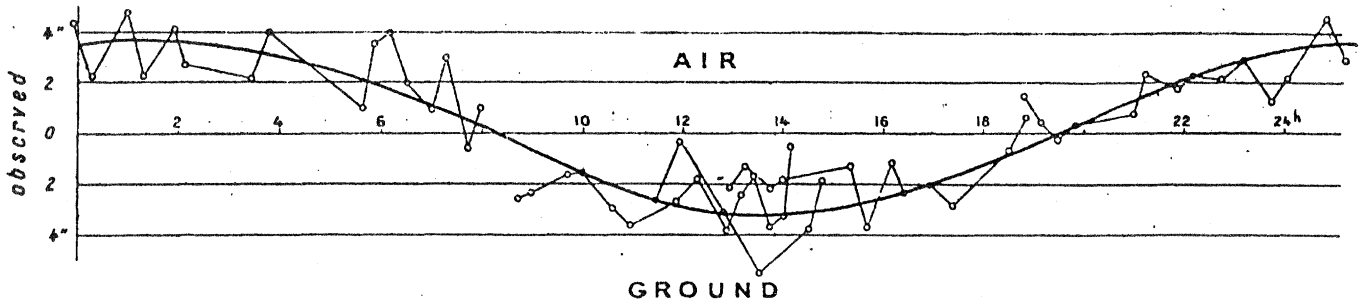

Figure 2.3 Effect of Lateral Refraction

during the day and 3" away from the ground at night. By taking temperature measurements along the line of sight, Kukkamaki was able to determine that the observed deflections were almost fully correlated with the horizontal temperature gradient. The only way to determine the horizontal temperature gradient is to observe the temperature along the line of sight, as Kukkamaki did. As this is not usually feasible in ordinary survey practice, the only recourse is to avoid situations where the line of sight passes close to a temperature anomaly, such as the wall of a building or a steep side slope.

From Chrzanowski [1977], the influence of centering error on an angle is given as

$$\sigma_c^2 = \rho^2 \left\{ \frac{\sigma_{c_1}^2}{D_1^2} + \frac{\sigma_{c_2}^2}{D_2^2} + \frac{\sigma_{c_3}^2}{D_1^2 D_2^2} (D_1^2 + D_2^2 - 2D_1 D_2 \cos a) \right\} \qquad (2\text{-}17)$$

where σ_{c_1} and σ_{c_2} = centering errors of the targets,

D_1 and D_2 = distances to the targets,

σ_{c_3} = centering error of the theodolite,

a = angle being measured,

ρ = 206265 .

For the case where the centering error of targets and instruments are about the same, and the distances are about equal, this reduces to

$$\sigma_{c_a}^2 = \frac{\rho^2 4\sigma_c^2}{D^2} \quad . \tag{2-18}$$

It should be noted that these expressions are for angles; for directions (2-18) becomes

$$\sigma_{c_d}^2 = \frac{\rho^2 2\sigma_c^2}{D^2} \quad . \tag{2-19}$$

As can be seen from the above expressions, the centering error's effect is largely dependent on the distance between target and instrument. For σ_c = 1 mm at a distance of 100 m, σ_{c_d} = 8".51.

The expected centering errors for different types of centering equipment (from Chrzanowski [1977] and Cooper [1977]) are listed in Table 2.3. This table assumes good conditions for centering (i.e. no wind for

Method of Centering	Expected Error (σ_c)
String plumb-bob	1 mm/m
optical plummet	0.5 mm/m
plumbing rods	0.5 mm/m
forced or self-centering	0.1 mm

Table 2.3 Expected Centering Error

the string plumb-bob and equipment in correct adjustment). These values are, of course, only approximate, and are also dependent on the particular equipment and the conditions under which they are used. For particular equipment and observers, the method for determining centering error outlined in section 2.1.4 should be used. Self centering refers to the method frequently used in traversing, i.e. leaving the tribrachs attached to the tripods and exchanging only the instrument and targets.

Tripod twist usually occurs when one side of the tripod is heated more than the other side. This twist can introduce a significant systematic error, especially for metal tripods (up to several arcsecs), and for precise work both the instrument and tripod should be shaded from direct sunlight.

2.3 Other Error Sources Encountered for Azimuths

When determining azimuths, either by gyro-theodolite or astronomical observations, other sources of error besides those already mentioned will affect the observations. These include timing inaccuracies, errors in star positions, and latitude dependent errors.

One must be careful when assessing the a priori accuracy of astronomic azimuths determined by star observations. Carter et al [1978] report that personal biases up to 1".1 have occured during astronomic azimuth determination in the United States. Thus, methods such as those outlined in section 2.1.4 must be used to ascertain these biases and eliminate them.

2.3.1 Gyro Azimuths

The azimuth as computed by a gyro-theodolite is given as

$$A = M - N + E \,, \qquad (2\text{-}20)$$

where A = astronomic azimuth,

M = horizontal circle reading for reference mark,

N = horizontal circle reading for north as determined by the gyro,

E = calibration value = difference between gyro determined astronomic north and true astronomic north.

The error in a gyro azimuth is

$$\sigma_A^2 = \sigma_M^2 + \sigma_N^2 + \sigma_E^2 \quad , \tag{2-21}$$

assuming no correlation between M, N and E. The element σ_M^2 is composed of reading, pointing, centering, etc. errors which have already been discussed. σ_N^2 and σ_E^2 are dependent on the inaccuracies resulting from determination of north by a gyro apparatus. Gregerson [1974] reports that these inaccuracies include mislevelment of the gyro, drift effects, changes in band torque equilibrium position, changes in angular momentum of the gyro, changes in the angle between the optical axis of the theodolite and axis of the gyro reading system, and changes in latitude ϕ. To characterize all these error sources and combine them into a single σ_N^2 or σ_E^2 would be a very large task, and when accomplished may not yield an accurate result. The most dependable way in which to determine the internal variance of a gyro azimuth is by calculating the variance of the mean of repeated determinations of the azimuth.

Some empirical accuracy estimates should, however, be mentioned. The expected accuracy for a gyro attachment such as the Wild GAK1 is about 20" to 30" [Bomford, 1975] in latitudes below 60°. Gyro-theodolites with automated recording of transit times (e.g. MOM Gi-B2 or GYMO-GI-B1/A) have an expected accuracy of about 3" for a single determination of azimuth

[Halmos, 1977].

If a gyro azimuth is to be used in an adjustment which is not 3 dimensional, it must be reduced by the truncated Laplace equation (assume $E_{ij} \simeq 90°$) to a geodetic azimuth as follows:

$$\alpha = A - \eta \tan \phi, \tag{2-22}$$

where α = geodetic azimuth,

A = astronomic azimuth,

η = prime vertical component of the deflection of the vertical,

ϕ = latitude of the point.

The variance of the geodetic azimuth α must reflect the inaccuracies in η and ϕ as well as the computed σ_A^2 (cf. section 2.4.5).

2.3.2 Azimuths Determined from Star Observations

These azimuths are usually determined by the hour angle or altitude methods. The azimuth by hour angle is

$$\tan A = \frac{\sin h}{\sin \Phi \cos h - \cos \Phi \tan \delta}, \tag{2-23}$$

where A = astronomic azimuth,

h = measured hour angle of star,

Φ = astronomic latitude of station,

δ = declination of star.

The expression for the variance of the astronomic azimuth based on the above equation, derived by Roelofs [1950], is

$$\sigma_A^2 = \frac{1}{n} F\sigma_t^2 + \frac{1}{n} (\sigma_p^2 + \sigma_c^2) \quad , \tag{2-24}$$

where n = number of pointings on the star,

σ_t^2 = variance of the observation of time in arcseconds (1" = 0.067 s),

σ_p^2 = variance of a single pointing on the star,

σ_c^2 = combined variance of 2 readings of the horizontal circle and pointing on the reference mark,

$F = \cos^2 \Phi \, (\tan \Phi - \cos A \cot Z)^2 + m(2 \tan^2 \Phi + \cot^2 Z - 2 \tan \Phi \cos A \cot Z)$,

Z = zenith angle of star,

$m = (\sigma_p^2 + \sigma_v^2)/\sigma_t^2$,

σ_v^2 = variance of levelling the spirit level.

The reading, pointing and levelling errors have all been discussed previously in section 2.1. The pointing error in this case is 70"/m because the star is a moving object. The only new source of inaccuracy here is the timing error. Mueller [1969] estimates σ_t = 0".5 with a chronograph and σ_t = 1".5 without a chronograph.

The determination of azimuth by star altitude does not require a precise knowledge of time. Here, both the horizontal and vertical circles are used, and the azimuth is computed as

$$\cos A = \frac{\sin \delta - \sin \Phi \sin a}{\cos \Phi \cos a} \quad , \tag{2-25}$$

where a = measured attitude corrected for refraction.

Roelof's [1950] equation for variance of the azimuth when using this method is

$$\sigma_A^2 = \frac{1}{n} \{(\sigma_p^2 + \sigma_v^2) \tan^2 a + (\tan \Phi - \cos A \tan a)^2$$

$$[(\sigma_{vc}^2 + \sigma_p^2) \operatorname{cosec}^2 A + \sigma_{tr}^2 \cos^2 \Phi] + (\sigma_p^2 + \sigma_c^2)\} , \quad (2\text{-}26)$$

where σ_{vc}^2 = combined variance of levelling vertical circle bubble and reading vertical circle,

σ_{tr}^2 = variance of tracking (ceasing to turn the telescope at the instant the star's image arrives at the intersection of the cross hairs) for simultaneous horizontal and vertical pointing on a star.

The variance of tracking is given by Mueller [1969] as $\sigma_{tr}^2 = 1''.0^2$, and σ_{vc}^2 will be the combination of the levelling and reading error for the vertical circle of the theodolite as discussed in section 2.1.

It should be noted that these variances characterize the random error of the internal accuracies of the azimuth determination. They do not account for the external errors such as refraction and centering error, which must also be accounted for when computing the final accuracy estimate.

The astronomic refraction will affect the altitude observation depending on the zenith angle of the star. Roelofs [1950] gives the refraction angle ε as

$$\varepsilon = \frac{p}{760} \cdot \frac{270}{270+t} \{60''.1 \tan Z - 0''.072 \tan^3 Z\}, \quad (2\text{-}27)$$

where p = pressure of the air (mm mercury) at the station,

t = temperature of the air (° Celcius) at the station.

Z = zenith angle of the star.

The corrected altitude a is then computed as

$$a = a' - \varepsilon, \tag{2-28}$$

where a' = measured altitude.

Thus, the external error resulting from refraction will be a result of inaccuracies in determination of temperature and pressure. Ignoring the last term in equation (2-27), their effect will be [Roelofs, 1950]

$$\sigma^2_{rf} = \left\{ \frac{1}{p^2} \sigma_p^2 + \frac{1}{(270 + t)^2} (\sigma_t^2 + \sigma_f^2) \right\} \left(\frac{p}{760} \cdot \frac{270}{270 + t} 60''.1 \tan Z \right)^2 , \tag{2-29}$$

where σ_p^2 = variance of reading the barometer,

σ_t^2 = variance of reading the thermometer,

and σ_f = mean short period fluctuation in temperature.

The mean short period fluctuation in temperature is taken as $\sigma_f = 0.2°C$. Equation (2-29) assumes that (2-27) is the exact model for the refraction angle ε. Although this is obviously not the case, Roelofs [1950] states that for zenith angles less than 75°, it will be sufficiently accurate.

It must be remembered that these are astronomic azimuths, and for obtaining geodetic azimuths α, equation (2-22) must be used. As well, for precise work, the gravimetric, skew-normal, and normal section to geodesic corrections must also be applied [e.g. Thomson et al., 1978]. Dracup [1975] uses the variance

$$\sigma_\alpha^2 = \sigma_A^2 + \left(\frac{\tan \phi}{0.8}\right)^2 + (0.4 \sin \phi)^2 \tag{2-30}$$

where σ_A^2 includes both internal and external errors, and the last two terms are generated by the corrective terms applied to the astronomic azimuth to get a geodetic azimuth. Equation (2-30) is also being used

in the 1978/79 readjustment of the maritime second order control networks for a priori geodetic azimuth weights [Chamberlain, 1978].

When working on a plane, the geodetic azimuth must be reduced to the mapping plane azimuth t by subtracting meridian convergence γ and (T - t) corrections [e.g. Thomson et al, 1978]. Thus, any inaccuracies in γ or (T - t) must also propogate into the variance of t, i.e.

$$\sigma_t^2 = \sigma_\alpha^2 + \sigma_\gamma^2 + \sigma_{(T-t)}^2 . \qquad (2\text{-}31)$$

2.4 Summary

This section summarizes the findings of the first 3 sections. The subsections are grouped under individual observation types, and each observation type is composed of both internal and external random error sources. Redundant observations are also accounted for.

2.4.1 Directions

The internal variance for a single direction is

$$\sigma_{d_i}^2 = \sigma_p^2 + \sigma_r^2 + \sigma_L^2 , \qquad (2\text{-}32)$$

where the pointing, reading, and levelling error are computed by equations (2-1) to (2-6). From (2-19) the external error is

$$\sigma_{d_e}^2 = \sigma_{c_d}^2 = p^2 \frac{2\sigma_c^2}{D^2} .$$

The variance of a single direction observation is

$$\sigma_d^2 = \sigma_p^2 + \sigma_r^2 + \sigma_L^2 + p^2 \frac{2\sigma_c^2}{D^2} . \qquad (2\text{-}33)$$

For n observations of the same direction, the variance changes according to the observing procedure used. If, as is usually done,

the zero setting is changed between "sets" of directions, with no relevelling or recentering of the instrument between sets, the final variance is

$$\sigma_d^2 = \frac{(\sigma_p^2 + \sigma_r^2)}{n} + \sigma_L^2 + \rho^2 \frac{2\sigma_c^2}{D^2} \quad . \qquad (2\text{-}34)$$

If, however, the instrument is relevelled and recentered (after turning instrument and targets through a 120° rotation) between sets, the final variance is

$$\sigma_d^2 = \frac{(\frac{\sigma_p^2 + \sigma_r^2}{2}) + \sigma_L^2 + \frac{\rho^2 2\sigma^2}{D^2}}{\frac{n}{2}} \quad , \qquad (2\text{-}35)$$

as there are 2 pointings and readings of the same direction within each set.

2.4.2 Horizontal Angles

Horizontal angles are essentially the difference of 2 directions. Thus, the variance of a single angle derived from 2 single directions is

$$\sigma_a^2 = 2\sigma_d^2 = 2(\sigma_p^2 + \sigma_r^2 + \sigma_L^2) + \frac{\rho^2 4\sigma_c^2}{D^2} \quad , \qquad (2\text{-}36)$$

where the final term could be replaced by equation (2-17) if it is expected that the centering error will be an important factor.

If, as is usually done, the angles are derived from direction observations, then n observations of an angle correspond to n observations of 2 directions, and the usual equation for the variance of angles is

$$\sigma_a^2 = 2\{\frac{\sigma_p^2 + \sigma_r^2}{n} + \sigma_L^2 + \frac{\rho^2 2\sigma_c^2}{D^2}\} \quad , \qquad (2\text{-}37)$$

corresponding to the same observation procedure that led to equation (2-34).

One must be careful about the covariance between angles which are derived from a set of more than 2 directions. If the situation exists as in Figure 2.4, then the angles a_{ijk} and a_{ikl} are usually derived as

$$a_{ijk} = d_{ik} - d_{ij} \quad , \qquad a_{ikl} = d_{il} - d_{ik} \quad . \tag{2-38}$$

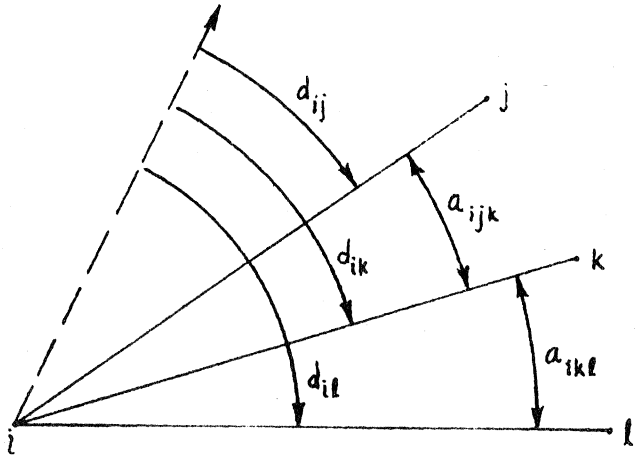

Figures 2.4 Angles and Directions

The propagation of errors from the directions into the angles by the covariance law yields the variance covariance matrix of the angles as

$$C_a = \begin{bmatrix} \sigma_{d_{ij}}^2 + \sigma_{d_{ik}}^2 & -\sigma_{d_{ik}}^2 \\ -\sigma_{d_{ik}}^2 & \sigma_{d_{ik}}^2 + \sigma_{d_{il}}^2 \end{bmatrix} . \tag{2-39}$$

One can see that because of the common direction d_{ik} between the 2 angles, the covariance - $\sigma_{d_{ik}}^2$ occurs. Thus, if angles are computed as above, the a priori variance covariance matrix is not diagonal, but has the off diagonal covariance terms of minus the variance of the common direction between individual angles.

Of course, it is possible to measure angles independently, and in this case no covariance terms will appear in C_a.

2.4.3 Zenith angles

Zenith angles can be considered the difference of 2 directions as well, one being defined by the vertical axis of the theodolite, the other by the optical axis of the telescope pointed at the target. The internal variance of a zenith angle is

$$\sigma_{z_i}^2 = \sigma_v^2 + \sigma_p^2 + \sigma_r^2 , \qquad (2\text{-}40)$$

where σ_v^2 is now the levelling error corresponding to the vertical circle index.

The external error is

$$\sigma_{z_e}^2 = \sigma_\varepsilon^2 + \sigma_\delta^2 , \qquad (2\text{-}41)$$

where σ_ε^2 is given by equation (2-12), and

$$\sigma_\delta^2 = \frac{\sin^2 E}{s^2} \sigma_{HT}^2 , \qquad (2\text{-}42)$$

for a variance σ_{HT}^2 of height of target and measured zenith angle E. Combining equations (2-40) and (2-41), and accounting for n zenith angle observations,

$$\sigma_{z_{..}}^2 = \frac{\sigma_v^2 + \sigma_p^2 + \sigma_r^2}{n} + \sigma_\epsilon^2 + \sigma_\delta^2 \quad , \qquad (2\text{-}43)$$

if the vertical circle index is relevelled for each observation. In most cases, the greatest source of inaccuracy is σ_ϵ^2.

2.4.4 Astronomic Azimuths

As already discussed, astronomic azimuths can be split by method of determination into 2 groups. For gyro azimuths, the internal variance is best calculated as the variance of the mean of repeated determinations, and for azimuths determined by star observations, they are given by equations (2-24) and (2-26), respectively. The external error is composed of centering error and, for azimuth determination by altitude of stars, the error in determination of astronomic refraction (equation (2-29)). Thus

$$\sigma_A^2 = \sigma_{A_i}^2 + \sigma_{c_d}^2 + \sigma_{rf}^2 \quad , \qquad (2\text{-}44)$$

where $\sigma_{rf}^2 = 0$ for gyro azimuths and azimuth by hour angle of stars. The accuracy increase for n observations is accounted for in the internal accuracy component.

2.4.5 Geodetic Azimuths

The geodetic azimuth α has further inaccuracies resulting primarily from the random error in the prime vertical component of the deflection of the vertical η (see equation (2-22)). An expression such as equation (2-30) must be employed to account for these inaccuracies.

2.4.6 "Grid" Azimuths

For grid or plane azimuths, equation (2-31) should be employed, but σ_γ^2 and $\sigma^2_{(T-t)}$ are usually very small in comparison with σ_α^2. In all practical cases, the variance of the grid azimuth can be assumed identical to that of the geodetic azimuth, namely

$$\sigma_t^2 = \sigma_\alpha^2 \qquad (2\text{-}45)$$

3. DISTANCE MEASUREMENTS

The accuracy of distance measurements is also divided into an internal and external component. Most distances are now observed with EDM, and the so-called zero and parts per million error are essentially internal and external errors, respectively. Both mechanical and optical methods of distance measurement are also considered as they are still widely used for distance observation.

3.1 EDM

Electromagnetic distance measuring (EDM) equipment utilize the following general equation for measured distance S:

$$S = \frac{1}{2} \lambda \, (m + \theta/2\pi) , \qquad (3\text{-}1)$$

where S = measured distance,

λ = modulation wavelength of frequency being used,

m = integer number of wavelengths in twice the distance,

θ = phase difference between transmitted and reflect wave in radians.

Thus, the variance of the measured distance for EDM is primarily a function of the variance of λ and θ (m is considered known), namely:

$$\sigma_S^2 = \{\frac{1}{2}(m + \theta/2\pi)\}^2 \sigma_\lambda^2 + \{\frac{1}{2}\frac{\lambda}{2\pi}\}^2 \sigma_\theta^2 . \qquad (3\text{-}2)$$

From equation (3-2), it is seen that the variance of determining the modulation wavelength λ contributes to the external variance (distance dependent), and the phase difference uncertainty σ_θ contributes to the internal variance. Other sources of inaccuracy such as zero error, error in zenith angle determination, and earth curvature determination error affect the final distance measurement, but the variance of the observed distance is basically characterized by equation (3-2).

3.1.1 Internal

The magnitude of σ_θ is primarily a function of the method used to determine the phase difference θ. In older EDM instruments, a phase discriminator circuit or CRT was used to indicate directly the difference in phase of the transmitted and received waves. In this case, a resolution of 0.01 of a cycle is possible [Burnside, 1971]. Instruments using null point methods of phase comparison [e.g. Geodimeter Model 6) can, as a general rule, detect a phase change of 0.001 of a cycle. The more recent digital method of phase detection, which is used largely in the modern infra-red equipment, gives a resolution from 0.001 up to 0.0003 of a cycle [Deumlich, 1974]. Table 3.1, from Deumlich [1974], points out the major features of some of the available modern EDM equipment.

The second term in equation (3-2) is due to inaccuracy in phase determination, and is rewritten as:

$$\sigma_{ph}^2 = \{\frac{1}{2}\lambda\}^2 \sigma_\theta^2 , \qquad (3\text{-}3)$$

for σ_θ in fractions of a cycle (i.e. parts of one wavelength).

Model	Manufacturer	Radiation Source	Modulation Frequency		Modulator	Power Consumed (W)	Method of Phase Measurement	Range (Km)		Standard Deviation
			Base (MH_Z)	Total #				Day	Night	
Geodimeter Model 8	AGA Sweden	5mW He-Ne Laser	30	4	KDP Crystal	75	null meter	30	60	$\pm$ (5 mm + 1 . 10^{-6}s)
Geodolite 3 G	Spectra-Physics U.S.A.	5mW He-Ne Laser	49	5		400	digital	60	80	$\pm 1.10^{-6}$s or 1 mm whichever greater
Geodimeter Model 6	AGA Sweden	30 W Mercury Lamp	30	3	Kerr Cell	70 300	resolver null meter	3 5	15 25	$\pm$(1 cm + 2.10^{-6}s)
Geodimeter 76	AGA Sweden	2mW Laser		2	Kerr Cell			3 (3 prisms)		$\pm$(1 cm + 1.10^{-6}s)
DM 1000	Kern	GaAs-Diode 900 nm	15	2	-	11	digital	2.5 (3 Refl.)		$\pm$ 1 cm
Mekometer ME 3000	Kern	Xenon-flash (100 Hz)	500	5	ADP Crystal	18	optomechanical null meter	3 (3 prisms)		$\pm$(0.2 mm + 1.10^{-6}s)
DM 500	Kern	GaAs Diode 875 nm	15	2	-	11	digital	0.5 (3 prisms)		$\pm$ 1 cm
SM 11	Zeiss Oberkochen	GaAs Diode 910 nm	15	2	-	12	automatic digital	2 (19 prisms)		$\pm$ 5 to 10 mm
ELDI 2	Zeiss Oberkochen					4		5		$\pm$ 5 mm
MA 100	Tellurometer	GaAs Diode 930 nm	75	4	-	14	digital	2		$\pm$(1.5 mm + 2.10^{-6}s)
CD 6	Tellurometer	GaAs Diode					digital	2		$\pm$(5 mm + 5.10^{-6}s)
SDM-3	Sokkisha Ltd, Tokyo	GaAs Diode 900 nm	15	2	-	10	digital	1 (3 prisms		$\pm$ 1 cm
DI 3	Wild Heerbrugg	GaAs Diode 875 nm	7.5	2	-	14	digital	0.6 (3 prisms)		$\pm$(5 mm + 5.10^{-6}s)
DM-60 Cubitape	Cubic Ind. Co., USA	GaAs Diode 900 nm	75	3	-	15	automatic digital	2		$\pm$(5 mm + 1.10^{-5}s)
3800 B	Hewlett-Packard, USA	GaAs Diode	15	4	-	12	digital null meter	3 (3 prisms)		$\pm$(5 mm + 1.10^{-5}s)
Ranger II	Laser Syst. & Electronics USA	3mW He-Ne Laser	15	4	KDP Crystal		automatic digital	6		$\pm$(5mm + 2.10^{-5}s)

Table 3.1 EDM Instruments

Model	Manufacturer	Carrier Frequency (GH_z)	Measuring Frequency (MH_z)	Antenna		Power Consumed (w)	Readout	Measuring Range (Km)	Standard Deviation
				Diameter (cm)	Divergence (°)				
MRA 101	Tellurometer Ltd.	10.05 to 10.45	7.5	33	6	38	digital	0.1 to 50	$\pm(1.5\ cm + 3.10^{-6}s)$
MRA 3	Tellurometer Ltd.	10.025 to 10.45	7.5	33	9		digital	0.1 to 50	$\pm(1.5\ cm + 3.10^{-6}s)$
MRA 4	Tellurometer Ltd.	34.5 to 35.1	75	33	2		digital	0.05 to 60	$\pm(3\ mm + 3.10^{-6}s)$
CA 1000	Tellurometer Ltd.	10.1 to 10.45	19 to 25				digital	0.05 to 30	$\pm(1.5\ cm + 5.10^{-6}s)$
Electrotape DM20	Cubic Corp. U.S.A.	10.5 to 10.5	7.5	33	6		digital	0.05 to 50	$\pm(1\ cm + 3.10^{-6}s)$
Distomat DI50	Wild Heerbrugg	10.2 to 10.5	15	36	6	50	digital	0.1 to 50	$\pm(2\ cm + 5.10^{-6}s)$
Distomat DI60	Siemens-Albiswerk	10.3	150	35	6	38	digital	0.02 to 150	$\pm(1\ cm + 3.10^{-6}s)$

Table 3.1 continued

For an instrument with modulation frequency 15 MHZ ($\lambda \simeq 20$ m), and a resolution $\sigma_\theta = 0.001$ of a cycle, $\sigma_{ph}^2 = 1.10^{-4}\ m^2$, or $\sigma_{ph} = 1$ cm.

Some instruments (e.g. the Wild DI-3) take the mean of a great many determinations of θ before employing equation (3-1) to determine the distance. In this instance, equation (3-3) reduces to

$$\sigma_{ph}^2 = \frac{1}{n} \{\frac{1}{2}\lambda\}^2 \sigma_\theta^2 \quad , \qquad (3\text{-}4)$$

where m is the number of determinations of the phase difference θ.

From the above discussion, it is seen that it is important to know the value of σ_θ^2 to obtain a reasonable estimate for σ_{ph}^2. A more accurate figure for σ_θ^2 than that which can be gleaned from the explanation above and Table 3.1 should be available (for a specific instrument) from the manufacturer's specifications.

One other source of internal error which must be considered is the uncertainty in the zero error σ_z which results from inaccurate knowledge of the difference between the electrical centre of the instrument and the point used to center the instrument over the station. For instruments using light waves, this value is usually negligible, but for microwave devices, the value can be quite significant. The zero error is dependent on the carrier frequency used; for instance in the MRA4 which has a carrier wavelength of 8 mm, σ_z is estimated at 3 mm, but for the MRA 101 (carrier wavelength of 3 cm), σ_z is thought to be closer to 15 mm [Burnside, 1971]. One method for determining the zero error on a calibrated baseline is given in Chrzanowski [1977].

3.1.2 External

The first term in equation (3-2) is due to the uncertainty in the determination of the modulation wavelength λ. Difficulties arise here primarily due to the index of refraction n, which affects the wavelength as

$$\lambda = \frac{\lambda_o}{n} \quad , \tag{3-5}$$

where λ_o is the wavelength resulting from

$$\lambda_o = \frac{c}{f} \quad , \tag{3-6}$$

for c = speed of light in a vacuum = 299792458 m/sec [Laurila, 1976], and f = modulation frequency being used.

Assuming λ_o to be errorless, the variance of λ is then given as

$$\sigma_\lambda^2 = \{\frac{\lambda_o}{n^2}\}^2 \sigma_n^2 \, . \tag{3-7}$$

Substituting this result back into the first term of equation (3-2) yields

$$\{\frac{1}{2}(m + \theta/2\pi)\}^2 \sigma_\lambda^2 = \{\frac{\frac{1}{2}\lambda_o (m + \theta/2\pi)}{n^2}\}^2 \sigma_n^2 = S^2 \frac{\sigma_n^2}{n^2} \quad , \tag{3-8}$$

where S is the distance being observed.

The refractive index n depends on the type of carrier wavelength used by the instrument. The two basic carrier wavelengths used by EDM are lightwaves (infra-red is also included here) and microwaves, and thus n and σ_n^2 are computed differently for these two cases.

For lightwaves, the formula of Barell and Sears is usually used as follows [Burnside, 1971]:

$$(n-1) = (n_G-1).\ \frac{273.15}{T}\ .\ \frac{P}{760} - \frac{15.02\ e}{T}\ .\ 10^{-6}\ , \qquad (3\text{-}9)$$

where T = temperature in degrees Kelvin (t°C + 273.15),

P = pressure of the air in mm Hg,

e = water vapour pressure in mm Hg,

n_G = refractive index for the group velocity defined as

$$(n_G-1)\ .\ 10^8 = 28760.4 + \frac{488.64}{\lambda_c^2} + \frac{6.80}{\lambda_c^4}\ , \qquad (3\text{-}10)$$

where λ_c = carrier frequency wavelength. For computation of e, one is referred to Bomford [1975 , p. 54]. Laurila [1976] arrives at the simplication

$$N = \frac{N_G P - 41.8\ e}{3.709\ T}\ , \qquad (3\text{-}11)$$

for $N = (n-1)\ .\ 10^6$, $N_G = (n_G-1).10^6$, and P and e in millibars. When evaluated for the effects of P, e and t, equation (3-11) gives

$$\sigma_N^2 = \{\frac{1}{T^2}\ (\ \frac{N_G}{3.709}\ P + 11.27\ e)\}^2\ \sigma_T^2 + \{\frac{N_G}{3.709\ T}\}^2\ \sigma_P^2 + \{\frac{11.27}{T}\}^2\ \sigma_e^2\ . \qquad (3\text{-}12)$$

Thus, σ_n^2 is computed as

$$\sigma_n^2 = \sigma_N^2\ .\ 10^{-12}\ . \qquad (3\text{-}13)$$

For microwaves, the group velocity is essentially equal to the carrier velocity, and the Essen and Froome formula is usually employed as follows:

$$N = \frac{77.62}{T}\ P - (\frac{12.92}{T} - \frac{37.19\cdot 10^4}{T^2})\ e\ , \qquad (3\text{-}14)$$

where T is in degrees Kelvin, P and e are in units of millibars, and $N = (n-1) \cdot 10^6$. The propogation of variance through equation (3-14) yields

$$\sigma_N^2 = \{\frac{-77.62}{T^2} + (\frac{12.92}{T^2} - \frac{74.38 \cdot 10^4}{T^3})\, e\}^2 \sigma_T^2 + \{\frac{77.62}{T}\}^2 \sigma_P^2 + \{\frac{-12.92}{T} + \frac{37.19 \cdot 10^4}{T^2}\}^2 \sigma_e^2 \quad (3\text{-}15)$$

Equation (3-15) is also due to Laurila [1976].

Table 3.2 from Kukkamaki [1967] summarizes the effects of errors

METEOROLOGICAL ERROR	EFFECT ON DISTANCE	
	Light Waves	Microwaves
± 1 mm Hg in air pressure	0.3 ppm	0.3 ppm
± 1°C in temperature	1.0 ppm	1.6 ppm
± 1°C in the difference between dry and wet bulbs	0.05 ppm	8.0 ppm

Table 3.2 Effect of Meteorological Errors on Measured Distances

in meteorological measurements on the measured distance. For light waves, the most important is temperature and air pressure, but for microwaves, the difference between wet and dry bulb temperatures, which is used to compute e, must be determined accurately.

Another external effect which cannot be overlooked is the error caused by reducing the measured slope distance S (already corrected for index of refraction and zero error) to either i) a horizontal distance S_h at the average height of the two stations (usually the procedure for localized surveys), or ii) the geodesic distance on a reference ellipsoid S_o.

Figure 3.1 [Chrzanowski, 1977] illustrates the individual steps in the reduction process.

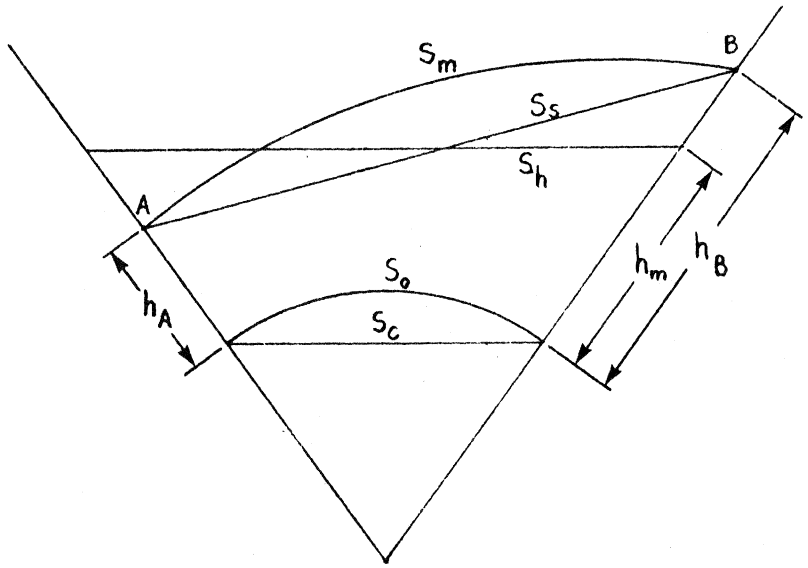

Figure 3.1 Reduction of Distances

There are essentially five separate corrections which must be considered in order to understand the errors resulting from them, and they are defined as follows [Bomford, 1975]:

1. The correction for the effect of curvature of the path of the ray and earth on the computation of the index of refraction. This correction is given as

$$\Delta S_1 = S_m - S = \frac{-S^3}{12R^2}(K - K^2) \quad , \tag{3-16}$$

where R = mean radius of the earth = 6370 km,

and K = R/κ, where κ is the radius of curvature of the path of the ray from A to B.

Under average conditions, κ=7R for lightwaves (K=1/7=0.143) and κ= 4R for microwaves (K=1/4=0.25).

2. Reduce the path distance S_m to the chord or spatial distance S_s. The latter would be the distance required for a three dimensional adjustment, and the correction is

$$\Delta S_2 = S_s - S_m = - \frac{S_m^3}{24R^2} K^2 . \qquad (3\text{-}17)$$

3. The correction ΔS_3 reduces the spatial distance S_s to the level distance S_h at the average height of the two points. The correction is

$$\Delta S_3 = S_h - S_s = - \frac{\Delta h^2}{S_m} - \frac{\Delta h^4}{8S_m^3} , \qquad (3\text{-}18)$$

where $\Delta h = (h_B - h_A)$ = difference in height between the two points.

4. The level distance S_h is reduced to the chord distance S_c at the ellipsoid by the correction

$$\Delta S_4 = S_c - S_h = \frac{S_h h_m}{(R_\alpha + h_m)} ,$$

where $h_m = \frac{1}{2} (h_A + h_B)$ = average height of the two points above the ellipsoid,

R_α = Euler radius of curvature for the line.

5. The final reduction of S_c to the geodesic distance S_o is via the correction

$$\Delta S_5 = S_o - S_c = \frac{S_m^3}{24R^2} . \qquad (3\text{-}20)$$

Thus, the reduced level distance S_h is

$$S_h = S = \Delta S_1 + \Delta S_2 + \Delta S_3 , \qquad (3\text{-}21)$$

and the final geodesic distance on the ellipsoid is

$$S_o = S_h + \Delta S_4 + \Delta S_5 . \qquad (3\text{-}22)$$

The effect of inaccuracies in the corrections ΔS propogate directly into the reduced distance S_h or S_o. By calculating a few examples, it can be seen that for distances under 50 km, the combined correction $\Delta S_1 + \Delta S_2$ is less than 1 ppm, and thus any inaccuracies in K, R, or S will not affect the reduced distance significantly. However, the correction ΔS_3 is directly linked to the difference in height, and any uncertainty in Δh will affect the correction ΔS_3 in the following way:

$$\sigma^2_{\Delta S_3} = \{\frac{\Delta h}{S_m}\}^2 \sigma^2_{\Delta h} \quad , \tag{3-23}$$

ignoring the small contribution of the second term (see equation (3-18)). For instance, for a distance S_m = 2000m, Δh = 100 m, and $\sigma_{\Delta h}$ = 0.5 m, $\sigma_{\Delta S_3}$ = 2.5 cm.

An important consideration here, then, is the method used to determine Δh. One of the usual methods employed is the measurement of the vertical or zenith angles to determine Δh as

$$\Delta h = S_s \cos E \quad , \tag{3-24}$$

where E is the measured zenith distance. An error σ_E in the zenith distance (see section 2.2.1) propagates as

$$\sigma^2_{\Delta h} = (S_s \sin E)^2 \sigma^2_E \quad , \tag{3-25}$$

which for a distance of 2000 m, E = 85°, and σ_E = 20" gives $\sigma_{\Delta h} \simeq$ 0.2 m.

The correction ΔS_4 will contribute an error of

$$\sigma^2_{\Delta S_4} = \{\frac{S_h}{R}\}^2 \sigma^2_{h_m} \quad , \tag{3-26}$$

where $(R + h_m)$ in equation (3-19) has been replaced by R. The height above the ellipsoid h_m is usually not well known due to inaccurate knowledge of the geoid height N. As can be verified from formula (3-26), each 6 m of error in h_m will contribute 1 ppm error to the reduced distance S_o.

3.1.3 Summary of Variance for EDM

The variance of the final reduced distance S_r is summarized as

$$\sigma_{S_r}^2 = \sigma_{ph}^2 + \sigma_z^2 + S^2 \frac{\sigma_n^2}{n^2} + \sigma_{\Delta S}^2 \quad . \tag{3-27}$$

The value to be used for $\sigma_{\Delta S}^2$ depends on the type of reduced distance desired. For the level distance S_h, $\sigma_{\Delta S}^2$ is equal to $\sigma_{\Delta S_3}^2$, and for the ellipsoidal distance S_o, $\sigma_{\Delta S}^2 = \sigma_{\Delta S_3}^2 + \sigma_{\Delta S_4}^2$ (see equations (3-23) and (3-26)). Distances to be used in a three dimensional adjustment will not require a $\sigma_{\Delta S}^2$ term unless they are exceptionally long (see section 3.2).

To understand how the variance is affected for more than one determination of the distance, one must first consider the normal observing procedure. Usually, the instrument is set up, the zenith angle is observed to determine Δh, the meteorological readings are taken, the distance is observed m_1 times, meteorological readings are taken again, the zenith angle is reobserved, and the procedure is complete. In this case, the variance of the reduced distance is

$$\sigma_{S_r}^2 = \frac{\sigma_{ph}^2}{m_1} + \sigma_z^2 + \frac{S^2 \sigma_n^2}{2n^2} + \frac{\sigma_{\Delta S}^2}{2} \quad . \tag{3-28}$$

Thus, the repeatedly observed distance serves only to reduce the variance of phase difference determination σ_{ph}^2. The uncertainty in the zero error is not affected and σ_n^2 and $\sigma_{\Delta S}^2$ are dependent on their individual measurement procedures. In general, for m_1 observations of phase difference, m_2 sets

of meteorological readings and m_3 determinations of the height differences,

$$\sigma_{S_r}^2 = \frac{\sigma_{ph}^2}{m_1} + \sigma_z^2 + \frac{S^2 \sigma_n^2}{m_2 n^2} + \frac{\sigma_{\Delta S}^2}{m_3} \quad . \tag{3-29}$$

Most instrument manufacturers state their instrument's accuracy as

$$\sigma_s = \pm (a + b.S) \quad , \tag{3-30}$$

where a and b are the internal and external standard deviations respectively. In the present context, $a = \sqrt{\sigma_{ph}^2 + \sigma_z^2}$ and $b = \sigma_n/n$. One can see that equation (3-30) is not valid, as

$$\sigma_S = \sqrt{\sigma_S^2} = \sqrt{a^2 + b^2 S^2} \neq a + bS \quad .$$

Equation (3-27) properly accounts for error propagation whereas equation (3-30) does not.

3.2 Mechanical Distance Measurement

Steel surveying tapes or chains as well as invar wires and tapes are considered here as the instruments used to measure distances mechanically. The errors in these measurements are all dependent on the distance measured, and thus are regarded as external errors.

For graduated steel tapes used with plumb bobs to determine the vertical, Kissam [1971] reports an expected accuracy of 1:2500 with no corrections applied, 1:3000 when using a spring balance to obtain the correct tension, and 1:5000 when the temperature correction is also applied.

Higher accuracy measurements are usually made with the tape suspended in catenary (see Figure 3.2). The ends of the tape are

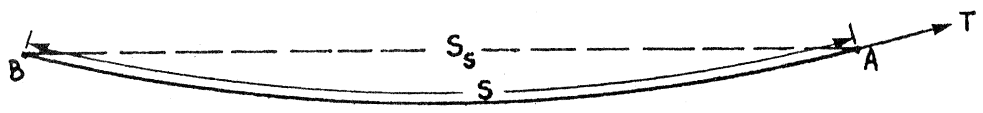

Figure 3.2 Tape in Catenary

supported firmly and precisely (usually by means of tripods designed for this purpose) at A and B, and a tension T (e.g. 10 Kg) is applied at A. The tape will then "sag" by a predictable amount (proportional to its weight per unit length, the distance between A and B, and the tension T) and the spatial distance S_s can be computed. A detailed analysis is contained in Bomford [1975].

Clark [1969] considers an accuracy of 1:20000 easily achievable with steel tapes in catenary which have been standardized (compared with an accurately known length) and which are used with applicable corrections (i.e. temperature, tension, sag and slope).

Invar wires or tapes in catenary can be used to obtain accuracies up to 1 to 2 ppm [Bomford, 1975]. Corrections considered necessary to achieve this accuracy (besides those mentioned above) include pulley friction, the weight of dirt or moisture on the wire or tape, the effect of wind, and the change in gravity between the standardisation site and measurement site. These high accuracy measurements with invar wires were primarily used to measure baselines to introduce scale to geodetic networks before the advent of modern EDM.

3.3 Optical Distance Measurement

Optical distance measurement is still an inexpensive and useful method of distance determination, even though it has been largely replaced by EDM. One reason for this is that the accuracy of optical distance measurement deteriorates quickly with increasing distance, even though relative accuracies up to 1:20000 are achievable for distances under about 500 m.

This section is based entirely on the comprehensive text "Optical Distance Measurement" by Smith [1970], and, as such, will summarize the main points pertaining to determination of the variance of the reduced distance. Of the nine separate types of optical distance measuring equipment covered by Smith [1970], only stadia tacheometry and subtense bars are considered here. As can be expected, errors here are related to those of Chapter 2 as these optical methods of distance measurement require theodolite observations.

3.3.1 Stadia Tacheometry

This method can be used on any theodolite which has stadia hairs. The reduced distance S_h is computed as (Figure 3.3)

$$S_h = Cb \cos\theta \cos\psi, \tag{3-31}$$

where C = instrument constant for stadia hairs (ususally 100),

b = difference in reading between upper and lower stadia hairs,

θ = observed vertical angle,

ψ = angle between normal to line of sight and the vertical rod.

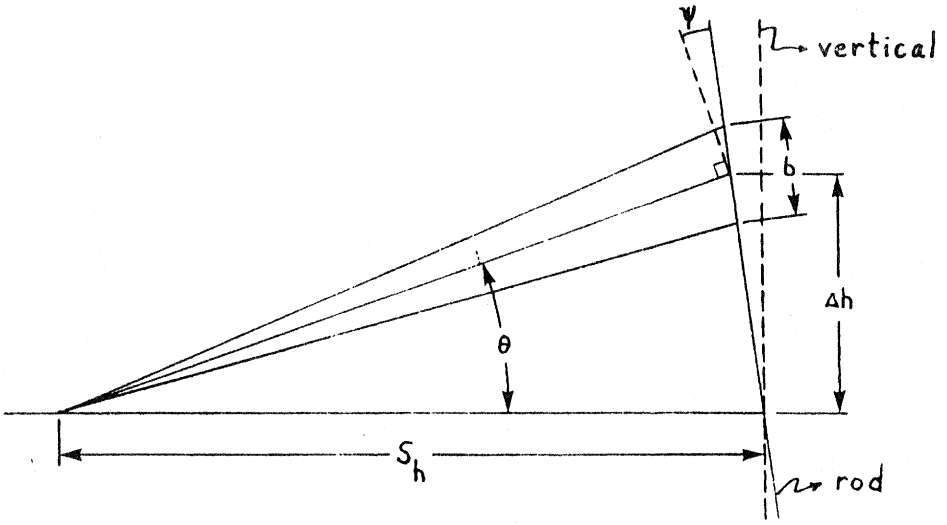

Figure 3.3 Stadia Measurements

The angle ψ is not taken equal to θ as the error σ_ψ in holding the rod vertically is not the same as the error σ_θ in the observed vertical angle. The error in the reduced distance is thus

$$\sigma_{S_h}^2 = \Delta h^2 \{\sigma_\theta^2 + \sigma_\psi^2\} + \{\frac{S_h \sigma_b}{b}\}^2 , \qquad (3\text{-}32)$$

where σ_θ and σ_ψ are in radians and Δh is the difference in height between the centre rod reading and the instrument station. The error in reading the rod σ_b is dependent on the pointing error (see section 2.1.1) and on the distance of the rod from the instrument. For example, given Δh = 8.7 m, S_h = 100 m, σ_θ = 1', σ_ψ = 1°, and σ_b = 0.7 mm, then σ_{S_h} = 0.167 m, which is a relative precision of 1:600.

The inaccuracy of vertical angle determination σ_θ has already been discussed in section 2.2.1, but it is obvious that σ_ψ will generally be the largest contributing factor. It is difficult to manually hold the rod vertically in error less than 1°, but if it could be aligned to 1', then the relative precision for the above example would be 1:1400.

3.3.2 Subtense Bar

The subtense bar method does not require a vertical angle observation; the horizontal distance is immediately available as (Figure 3.4)

$$S_h = \frac{b}{2} \cot \frac{a}{2} , \tag{3-33}$$

where b = length of the subtense bar,

a = measured horizontal angle subtended by the subtense bar.

The length of the bar b is well known (e.g. $\sigma_b = 0.00005$ m), and the primary source of error is σ_a^2, the variance of the measured angle. The evaluation of σ_a^2 is covered in section 2.4.2. The variance of the computed distance is

$$\sigma_{S_h}^2 = \{\frac{S_h^2 \sigma_a}{b}\}^2 , \tag{3-34}$$

for σ_a in units of radians.

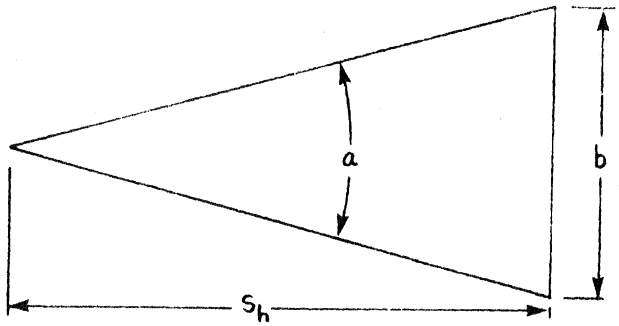

Figure 3.4 Bar at End

Differently configured setups yield different values for $\sigma_{S_j}^2$. If the subtense bar is set in the middle of the line as depicted in Figure 3.5, then the variance for S_h is

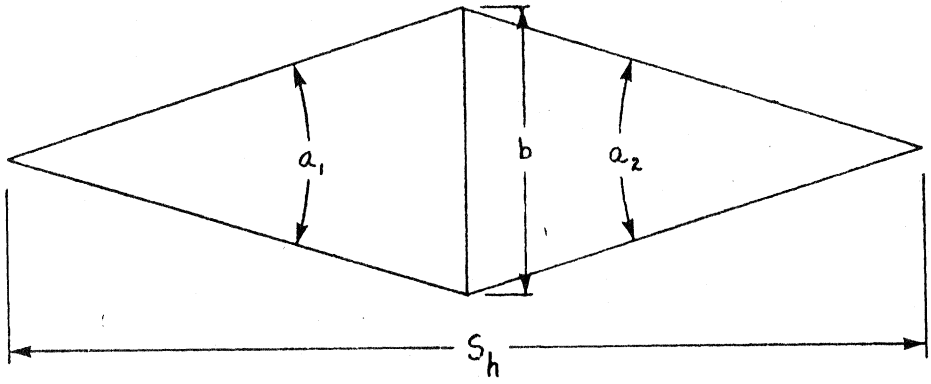

Figure 3.5 Bar in the Middle

$$\sigma_{S_h}^2 = \{\frac{S_h^2 \sigma_a}{2\sqrt{2}\, b}\}^2 , \tag{3-35}$$

which is 2.8 times better than for the bar at the end of the line. Equation (3-35) assumes $a_1 = a_2$ and $\sigma_{a_1} = \sigma_{a_2}$. In general, for n equal segments of shape as in Figure 3.4, the error is

$$\sigma_{S_h}^2 = \{\frac{S_h^2 \sigma_a}{b\, n^{3/2}}\}^2 . \tag{3-36}$$

For an auxiliary base at the end of a line, as depicted in Figure 3.6, the error in distance is

$$\sigma_{S_h}^2 = S_h^2 \{\frac{b'^2}{b^2} + \frac{S_h^2}{b'^2}\} \sigma_a^2 , \tag{3-37}$$

for σ_a in radians. The optimum condition (least error in S_h) occurs when

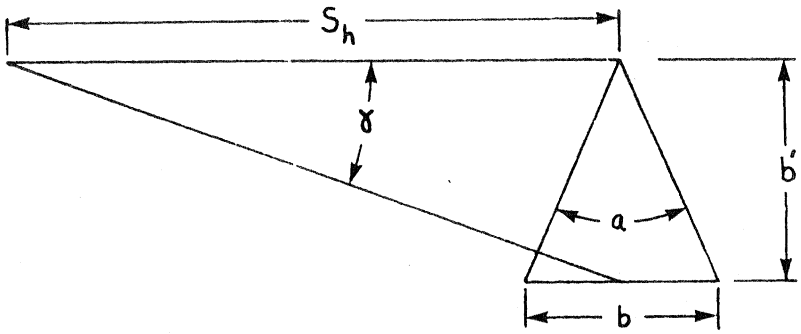

Figure 3.6 Auxiliary Base at End

$\gamma = a$ (see Figure 3.6), and in this case

$$\sigma^2_{S_h} = \frac{2\, S_h^3}{b}\ \sigma_a^2 \quad , \tag{3-38}$$

for σ_a in radians.

When the auxiliary base is placed in the middle of the line

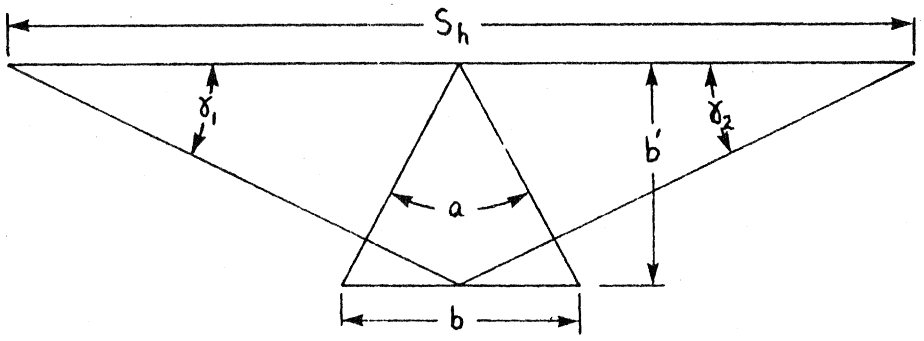

Figure 3.7 Auxiliary Base in the Middle of the Line

as in Figure 3.7, then

$$\sigma^2_{S_h} = S_h^2 \left\{\frac{b'^2}{b^2} + \frac{S_h^2}{8b'^2}\right\} \sigma_a^2 \quad , \tag{3-39}$$

again for σ_a in radians. Optimal conditions occur here for the ratio $a: \gamma_1 : \gamma_2 = \sqrt{2} : 1 : 1$, which yields

$$\sigma^2_{S_h} = \frac{2S_h^3}{2.8b}\ \sigma_a^2 \, . \tag{3-40}$$

Figure 3.8 [Smith, 1970] shows the relative precision expected for the four cases discussed above assuming a subtense bar of length b = 2 m.

3.4 Summary

This section summarizes the variance of the three types of distance measurement discussed above. Each method is treated independently of the others because of the unique nature of the individual distance determination procedures.

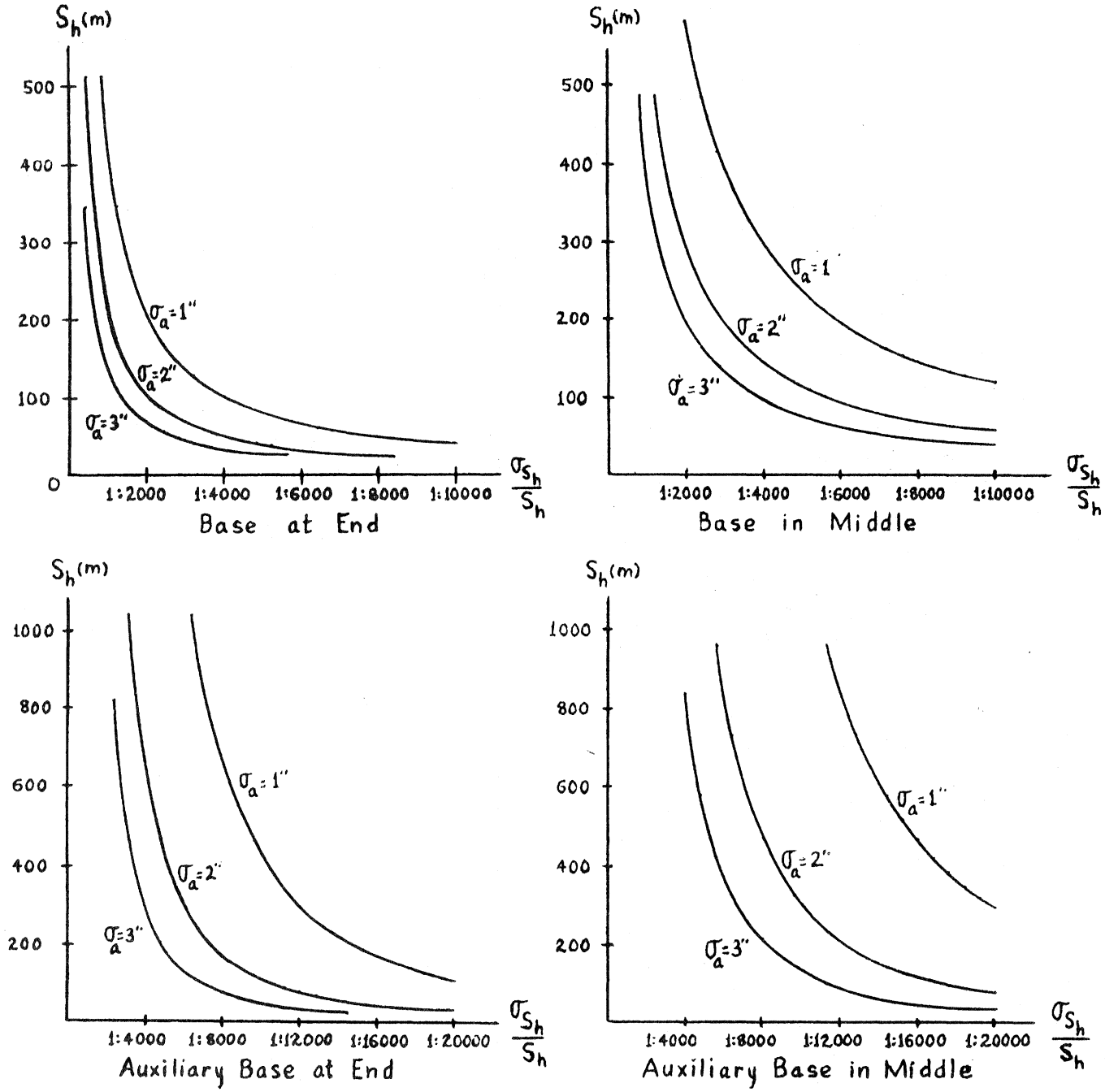

Figure 3.8. Expected Relative Precision of Subtense Bar Measurements

For EDM distances, the final variance is given by equation (3-29) as

$$\sigma_S^2 = \frac{\sigma_{ph}^2}{m_1} + \sigma_z^2 + \frac{S^2\sigma_n^2}{m_2 n^2} + \frac{\sigma_{\Delta S}^2}{m_3} \quad ,$$

where $\sigma_{\Delta S}^2$ depends on the type of reduced distance required (see section 3.1.3), σ_n^2 is computed by equation (3-12) or (3-15) depending on the carrier frequency wavelength, σ_z^2 is either given by the manufacturer or determined through a calibration procedure, σ_{ph}^2 is determined from equation (3-3) or (3-4), and m_1, m_2 and m_3 are as explained in section 3.1.3.

The variance of mechanical methods of distance observation is characterized by

$$\sigma_S^2 = S^2 \sigma_{S_m}^2 \qquad (3\text{-}39)$$

where σ_{S_m} is the relative precision of the method being used (see section 3.2). For example, consider taping carried out with plumb bobs and no corrections applied for tension or temperature; then $\sigma_{S_m}^2 = (1/2500)^2$, and for a measured distance of 500 m, $\sigma_s = 0.2$ m.

Optically determined distances have a variance which is highly dependent on the individual method used. For stadia tacheometry, equation (3-32) characterizes the variance, and for subtense bar measurements, equations (3-34), (3-35), (3-38) and (3-40) define the variances depending on the specific subtense method used. Each of these formulae depend on σ_a^2 (the variance of angle determination) which is given by equation (2-37).

REFERENCES

Angus-Leppan, P.V. 1961. Study of Refraction in the Lower Atmosphere. Empire Survey Review, Vol. XVI, Nos. 120, 121 and 122.

Angus-Leppan, P.V. 1971. Meteorological Physics Applied to the Calculation of Refraction Corrections. Paper, Commonwealth Survey Officers Conference.

Bomford, G. 1975. Geodesy. London: Oxford University Press.

Burnside, C.D. 1971. Electromagnetic Distance Measurement. London: Crosby Lockwood Staples.

Carter, W.E., J.E. Petty, and W.E. Strange. 1978. The Accuracy of Astronomic Azimuth Determinations. Bulletin Géodésique, Vol. 52, no. 2.

Chamberlain, C.A.M. 1977. Mathematical Models for Horizontal Geodetic Networks. Technical Report no. 43, Dept. of Surveying Engineering, University of New Brunswick, Fredericton.

Chamberlain, C.A.M. 1978. Personal Communication.

Chrzanowski, A. 1977. Design and Error Analysis of Surveying Projects. Lecture Notes no. 47, Dept. of Surveying Engineering, University of New Brunswick, Fredericton.

Clark, D. 1969. Plane and Geodetic Surveying for Engineers. Vol. 1, Plane Surveying, Sixth ed. London: Constable and Co-Ltd.

Cooper, M.A.R. 1971. Modern Theodolites and Levels. London: Crosby Lockwood & Son Ltd.

Deumlich, F. 1974. Instrumentenkunde der Vermessungstechnik. Berlin: VEB Verlag fur Bauwesen.

Dracup, J.F. 1975. Use of Doppler Positions to Control Classical Geodetic Networks. Paper, International Association of Geodesy, XVI General Assembly, Grenoble.

Faig, W. 1972. Advanced Surveying I. Lecture Notes no. 27, Dept. of Surveying Engineering, University of New Brunswick, Fredericton.

Gregerson, L.F. 1974. Using Gyrotheodolites for Precise Determination of Azimuth. Internal Report, Geodetic Survey of Canada.

Halmos, F. 1977. High Precision Measurement and Evaluation Method for Azimuth Determination with Gyro-theodolites. Manuscripta Geodetica, Vol. 2, no. 3, p. 213.

Kissam, P. 1971. Surveying Practice. Second ed. New York: McGraw Hill.

Kukkamaki, T.J. 1949. On Lateral Refraction in Triangulation. Bulletin Geodesique, no. 11.

Kukkamaki, T.J. 1967. Geodetic Refraction, Vertical Horizontal and Longitudinal. International Dictionary of Geophysics. London: Pergamon Press.

Laurila, S.H. 1976. Electronic Surveying and Navigation. New York: John Wiley & Sons.

Mepham, M.P. 1976. A Rigorous Derivation of Station Adjustment Formulae for Complete and Incomplete Sets. Report for SE 4711, Dept. of Surveying Engineering, University of New Brunswick, Fredericton.

Mepham, M.P. 1977. Short Line Trigonometric Levelling. Report for SE 3701 Dept. of Surveying Engineering, University of New Brunswick, Fredericton.

Mueller, I.I. Spherical and Practical Astronomy as Applied to Geodesy. New York: Frederick Ungar Publishing Co.

Pfeifer, L. 1975. Use of Ferrero's Formula to Estimate a Priori Variance of Horizontal Directions. Paper, I Venezuelan Congress of Geodesy, Maracaibo.

Ramsayer, K. 1978. The Accuracy of the Determination of Terrestrial Refraction from Reciprocal Zenith Angles. Paper, IAU Symposium 89, Refractional Influences in Astrometry and Geodesy, Uppsala.

Robbins, A.R. 1976. Military Engineering. Vol XIII, Part IX, Field and Geodetic Astronomy. Ministry of Defense.

Roelofs, R. 1950. Astronomy Applied to Land Surveying. Amsterdam: N.V. Wed. J. Ahrend & Zoon.

Smith, J.R. 1970. Optical Distance Measurement. London: Crosby Lockwood & Son Ltd.

Thomson, D.B., E.J. Krakiwsky and J.R. Adams. A Manual for Geodetic Position Computations in the Maritime Provinces. Technical Report no. 52. Dept. of Surveying Engineering, University of New Brunswick, Fredericton.

Vincenty, T. 1973. Three-Dimensional Adjustment of Geodetic Networks. Internal Report, DMAAC Geodetic Survey Squadron.